

# Compressible Coanda wall jet: predictions of jet structure and comparison with experiment

A. R. Gilchrist\* and D. G. Gregory-Smith

School of Engineering and Applied Science, University of Durham,  
Science Laboratories, South Road, Durham, DH1 3LE, UK

Received November 1986 and accepted for publication April 1987

A two-dimensional underexpanded jet blowing tangentially over a cylindrical surface was studied experimentally and reported in a previous paper. The curved jet has a shock cell structure similar to that of a plane jet, but with a separated region on the curved surface. This region grows with increasing upstream blowing pressure until reattachment fails to take place and the jet breaks away from the surface. This paper reports progress in calculating the jet structure so that predictions may be made of the jet development and of breakaway conditions. The inviscid core of the jet was calculated by the method of characteristics: the outer shear layer and surface boundary layer were ignored. When compared with experiments, this gave good predictions for the structure of the first shock cell for low blowing pressures. However, the neglect of the separated region on the surface caused increasing error in the predictions as blowing pressures increased. The program was modified to replace the wall condition by a specified pressure boundary, the pressures being obtained experimentally. The predictions then agreed well with experimentally observed flow patterns for the first one or two shock cells. After that the growth of the shear layer encroaches into the core so that the shock cell structure disappears. Although of wide application, this work is particularly related to the design of Coanda flares where the jet is axisymmetric. As well as extension of the method to axisymmetric geometry, further work is required to develop methods to predict the outer shear layer and the separated region. This would enable predictions of complete jet development and breakaway conditions to be made.

**Keywords:** Coanda effect; compressible wall jet; underexpanded jet; shock cells; method of characteristics

## Introduction

The Coanda effect is used to describe the phenomenon whereby a jet blown over a surface of convex streamwise curvature adheres to the surface. A previous paper by the authors<sup>1</sup> describes an experimental investigation into the jet structure of an underexpanded jet blown over such a curved surface. The particular application of the work was to the design of Coanda flares (see Figure 1) in which a jet of combustible gas emerges from a slot at the base of an axisymmetric tulip-shaped body. The jet adheres to the surface by the Coanda effect, and the curved jet has the important feature of high turbulence, which leads to a rapid entrainment of ambient air. Thus there is good premixing and efficient combustion with low radiation and low smoke pollution. These flares have been developed by British Petroleum plc and are described by Wilkins *et al.*<sup>2</sup> The Coanda effect has found many other applications, varying from small fluidic devices to reenergizing boundary layers on aircraft wings and jet flap devices.

In Coanda flares the gas supply pressure is usually above that required for choked flow, and so the issuing jet is underexpanded. If the supply pressure is raised sufficiently, the jet can break away from the surface to form a free jet. One of the main aims of the previous paper<sup>1</sup> was to investigate the

mechanism of breakaway. This was done by studying the curved two-dimensional jet, i.e., blowing over a cylindrical rather than axisymmetric surface. Using the optical techniques of schlieren and shadowgraph together with surface flow visualization and

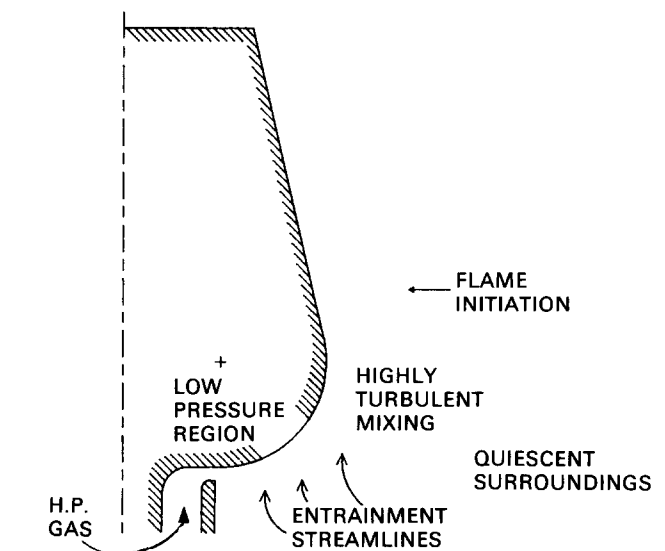


Figure 1 Principles of the Coanda flare

\* Formerly of the School of Engineering and Applied Science, University of Durham

static pressure tapings, we have identified the following features of the flow:

- (a) A shock cell structure existed that was similar to that of a plane free jet with successive regions of expansion and compression.
- (b) The shock cell structure disappeared more rapidly than with a plane free jet due to the more rapid growth of the outer shear layer caused by the streamwise curvature.
- (c) A separated region existed on the Coanda surface caused by the compression at the end of the first shock cell. This region was characterized by a stagnant pressure region followed by a region of strongly reversed flow before reattachment took place at the point where reexpansion started in the second cell.
- (d) The separated region modified the first shock cell structure, with the point of separation initiating a shock wave which became stronger as the upstream pressure was increased.
- (e) The separated region grew rapidly as the upstream pressure was increased, until reattachment failed to occur and the jet suddenly broke away from the surface.

For design purposes the calculation of the complete jet is ideally desirable, including the outer free shear layer, the central mainly supersonic core, and the boundary layer or separated region on the curved surface. This is a very complex task, but as regards the practically important phenomenon of breakaway the experimental results suggested that calculation of the first shock cell, ignoring the outer shear layer (which encroaches only slightly), could give an indication of when breakaway might occur. Thus the aim of the work reported in this paper was to develop a prediction technique for the first shock cell and to relate this to the breakaway conditions.

## Calculation method

### Background

Because of the presence of a substantial normal pressure gradient, the subsonic curved wall jet may not be treated as a parabolic phenomenon. However, the influence in the upstream direction is not strong, and Morrison and Gregory-Smith<sup>3</sup> produced a partially parabolic method for cylindrical or axisymmetric low-speed wall jets. The method was based on the GENMIX method of Spalding<sup>4</sup> and used simple modifications to the mixing length for curvature and divergence. Other workers, for example Gibson and Younis,<sup>5</sup> have used more sophisticated turbulence models. The above methods are designed to give the fully developed jet some distance downstream from the slot.

For high-speed jets, the shock cell structure close to the slot is very important, and as the shear layer grows the shock cells disappear and the jet becomes entirely subsonic. Dash *et al.*<sup>6</sup> have suggested approaching this problem by treating separately the inviscid core, the viscous outer shear layer, and the boundary layer on the wall. However, the problem of a separated region on the wall was not considered.

It was clear that for the application considered here, the structure of the first shock cell was of greatest importance. Thus the method of characteristics was chosen, because it is a well-tried and fast method for calculating supersonic flow. Various workers have used the method for underexpanded jets—for example, Chang and Chow<sup>7</sup> for the round jet and Benson and Poole<sup>8</sup> for the plane two-dimensional jet.

### Method of characteristics

The method of characteristics is well documented (e.g., Zuchrow and Hoffman<sup>9</sup>), so only an outline of the particular application is given here. Gilchrist<sup>10</sup> gives the method in detail. In irrotational flow there are two characteristics whose slope is given by

$$\left(\frac{dy}{dx}\right)_{\pm} = \tan(\theta \pm \alpha)$$

where  $\theta$  is the angle of the local streamline to the  $x$  axis and  $\alpha$  is the Mach angle defined by

$$\alpha = \sin^{-1}(1/M)$$

In rotational flow there is a third characteristic, the streamline. Rotational flow occurs after curved shock waves, but since the main interest was the first shock cell before any shock waves occur, the calculation program was written for irrotational flow.

The characteristic and compatibility equations were expressed in finite difference form and solved by the Euler predictor-corrector method. In the corrector step, the average property method as recommended by Hoffman<sup>11</sup> was chosen. For proceeding downstream, the direct marching method was used, whereby the left and right running characteristics are followed throughout the flow field, the solutions being obtained at their intersections. Thus the solution at any predetermined point must be interpolated from the grid generated by the characteristics. The alternative (inverse marching) is to obtain the solution at predetermined grid points by running characteristics back to the previous column and interpolating for the properties on the characteristic. Zuchrow and Hoffman<sup>9</sup> suggest that, in general, the direct marching method is more accurate because it eliminates the cumulative interpolation errors of inverse marching. It is also simpler to program and handles the free-jet boundary more easily.

The upstream boundary condition is the exit flow from the slot. For irrotational flow, the stagnation conditions must be uniform, but the local Mach number may be specified to vary. However, it must always be above unity, since the method of characteristics applies only to supersonic flow. On one side of the jet, there is the free-jet boundary, which is at a specified pressure (in this case, constant). Only one characteristic exists, but the extra equations required are obtained from the free-jet edge being a streamline and the velocity being given by an isentropic expansion from the inlet stagnation conditions to the specified boundary pressure.

On the other side of the jet, the solid surface is a boundary. This is easily treated since the surface is a streamline and its

### Notation

$a$	Radius of curvature of surface
$b$	Slot width
$M$	Mach number

$P_a$	Ambient pressure
$P_o$	Upstream stagnation pressure
$P_s$	Surface static pressure
$x, y$	Cartesian coordinates
$\alpha$	Mach angle
$\theta$	Angle of streamline to $x$ direction

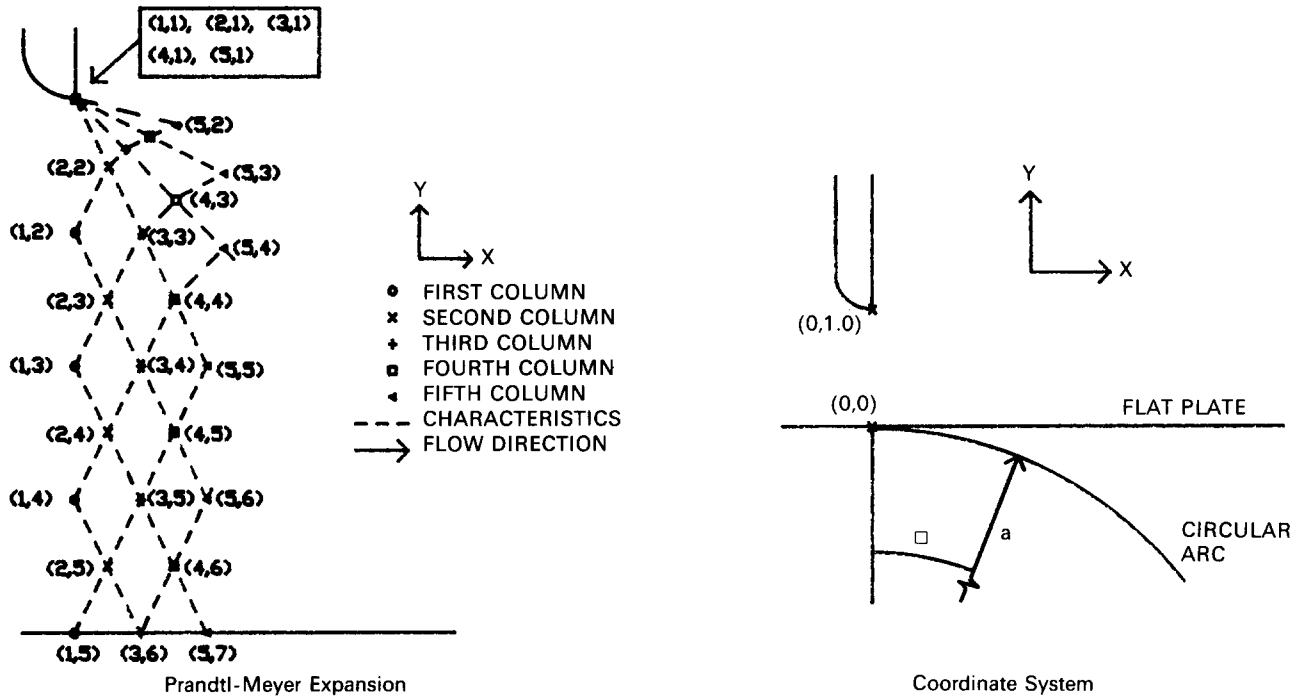


Figure 2 Method of characteristics

position is known. However, a modification to the method (see the last subsection of this section) was made, whereby the surface was replaced by a specified pressure distribution. The boundary was then treated in the same way as the free-jet boundary.

If shock waves occur, there are two methods which may be used to treat them. The first is the method of foldback, whereby the characteristics are allowed to fold back on top of one another. Eventually the solution marches downstream again, the flow being assumed irrotational throughout, and so the shock is effectively ignored. The second is to combine the standard oblique shock equations with the method of characteristics and to determine the shock position and strength iteratively. The flow downstream will be rotational if the shock is curved. Zuchrow and Hoffman<sup>9</sup> suggest that the foldback method yields reasonable results for "shocks," provided that the static pressure ratio across the real shock is less than 1.25. For this application, the foldback method was used.

**Computer program**

A computer program based on the above method was written in FORTRAN to calculate the two-dimensional supersonic jet over a flat or curved surface. It was written for a cartesian coordinate system, as shown in Figure 2.

The calculation starts on an initial column at the slot exit and calculates the properties along the column and the Prandtl-Meyer expansion centered on the nozzle lip edge, as shown in Figure 2. The Mach number along the first column at  $x=0$  can be specified as constant or linearly varying. A minimum Mach number of 1.02 was chosen, since the method of characteristics fails if the Mach becomes equal to unity. The Prandtl-Meyer expansion is modeled by propagating several expansion waves from the nozzle lip. The number of grid points is increased during this expansion, as shown in Figure 2. The first grid point of each column is held on the lip edge, and the expansion waves have an equal static pressure ratio drop across them. After the initial Prandtl-Meyer expansion, the number of solution points

in each column is kept constant, with alternate columns having a wall boundary and a free-jet boundary point.

For the flow over a curved surface, precautions have to be taken to ensure that no characteristic gradient approaches infinity. After each calculation of a column, a check is made, and, if necessary, the cartesian coordinate system is rotated through a specified angle.

In addition to property values at each grid point, the output contains a graphical picture of the expansion and compression waves. This is especially helpful in comparing results with the pictures obtained from the optical experiments. The program was run on an IBM 4341 computer. The run time depended on the number of columns calculated downstream, but was typically 60s of CPU time.

**Flat wall tests**

Computational tests were carried out on an underexpanded jet flowing over a flat wall downstream of the nozzle exit. This is equivalent to the plane free underexpanded jet investigated by Benson and Poole,<sup>8</sup> with the wall as the axis of symmetry. This provided a check on the program.

Tests were made to determine grid independency by varying the number of initial rows and the number of Prandtl-Meyer expansion waves. It was found that 20 initial rows with 11 Prandtl-Meyer waves gave effective grid independency.

Figure 3 shows the results for three different ratios of downstream pressure to upstream stagnation pressure. The diagrams follow the development of the expansion waves centered on the nozzle lip. These are initially straight until they meet a reflection of the first wave from the wall. The expansion waves reflect as expansion waves off the wall (or line of symmetry), and so the waves are curved in the region of interaction between the incident and reflected waves. The waves are reflected off the free boundary as compression waves to preserve constant pressure at the boundary. This causes the free boundary to curve back toward the wall. For the highest pressure ratio, the compression waves are reflected off the wall

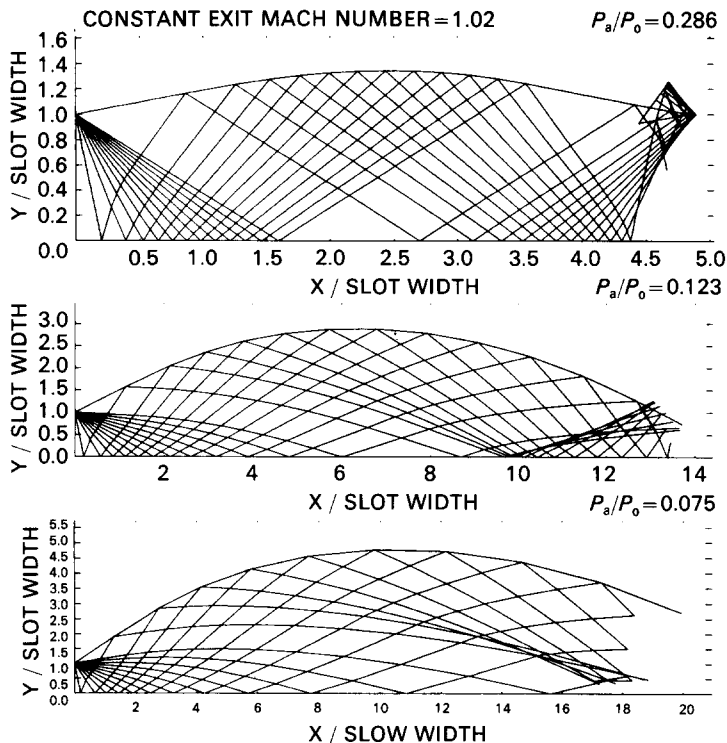


Figure 3 Jet over flat surface

before coalescing, thus indicating the presence of a weak oblique shock. This corresponds to the first shock type described by Benson and Poole<sup>8</sup> and discussed in the previous paper.<sup>1</sup> Downstream of the shock the calculation stops because part of the flow goes subsonic.

As the pressure ratio is reduced (blowing pressure increased), the maximum width and the length of the cell is increased. The compression waves coalesce earlier, the shock appears before the compression waves reach the wall, and the shock is reflected off the wall. This corresponds to the second shock type described by Benson and Poole. However, at the lowest stagnation pressure of Figure 3, Benson and Poole found the third shock type existed, with the oblique shock joining a normal shock across the central part of the jet (also known as a Mach disc in a round jet). This is not predicted here because of the simple treatment of shocks in the method.

A direct comparison with the results of Benson and Poole is difficult, because the conditions at their slot are not known precisely. However, the similarity of the results gave confidence that the program was functioning correctly.

Tests were made with a variation of Mach number at the initial column from 1.02 on the wall to a higher value at the nozzle lip. A typical result is shown in Figure 4, which had a lip Mach number of 1.4 and may be compared with the central diagram of Figure 3. Although the cell is slightly shorter and thinner, the differences are very slight. This was generally the case with other tests, and it was concluded that the effect of variable Mach number was not important. The reason for the tests was that in the experimental model the curvature of the upstream channel before the slot exit was expected to cause slightly nonuniform exit conditions. This was confirmed experimentally.<sup>1</sup>

**Modification of computer program**

As indicated above, the experimental results show that there is a region of separated flow on the curved surface. The basic program predictions for the jet do not give good results when

the separated region is substantial, as it is for high blowing pressures. Therefore the program was modified so that the wall condition (i.e., the flow remaining tangential to the surface) was replaced by a specified pressure boundary, the pressure value being obtained experimentally. The modified program initially calculates the jet with the original wall boundary, since the first measured static pressure tapping was 5° around the surface. At a chosen angle the boundary condition is switched to the specified pressure condition. The pressure is obtained by interpolating from the measured static pressures on the curved surface, with the assumption that the static pressure remains constant on an extended radius from the surface to the inner boundary of the jet. This assumption of constant static pressure normal to the surface through the separated region is likely to be acceptable, except perhaps for the largest separations as breakaway is approached.

The program outputs the jet shape and the interpolated and known surface static pressures. In some cases where the interpolation gave unreasonable values, it was necessary to correct them manually, especially near the start of separation where the streamwise pressure gradient suddenly changed.

**Curved wall-jet predictions**

*Attached jet results*

The program was run in its original form to give the predictions for the jet attached to the Coanda surface. Figure 5 shows the patterns for two pressure ratios and the static pressures on the surface for four pressure ratios. The patterns show the progression of the Prandtl-Meyer expansion waves as in Figure 3 for the flat plate. There are additional expansion waves originating from the Coanda surface. These are required to turn the flow around the curved surface, but for clarity they are not shown. The effect of these waves can be seen by the curvature of the Prandtl-Meyer waves before they interact with their first reflections off the surface. As with the flat plate, the lower pressure ratio gives a larger cell before the program stops due to subsonic flow. The lower pressure ratio pattern in Figure 5 is of the second shock type, with the shock wave forming before the compression waves reach the wall, and the shock is reflected off the surface. This gives the folded-back static pressure distribution for the lowest pressure ratio (0.238). Generally, the surface static pressure falls initially due to the surface expansion waves, but then there is a more rapid drop as the Prandtl-Meyer expansion waves arrive at the surface. The pressure continues to fall slowly after the last Prandtl-Meyer wave has been reflected, due to more surface expansion waves. The reflected Prandtl-Meyer waves off the free surface start to arrive as compression waves, and the pressure rises sharply. There is then a less sharp rise caused by the reflections (as compression waves) from the free surface of the expansion waves from the Coanda surface.

As with the flat surface, some tests were made with a nonuniform Mach number at exit from the slot. Again it was found that the effect was small (Gilchrist<sup>10</sup>), so all the results presented here are for a uniform exit Mach number of 1.02.

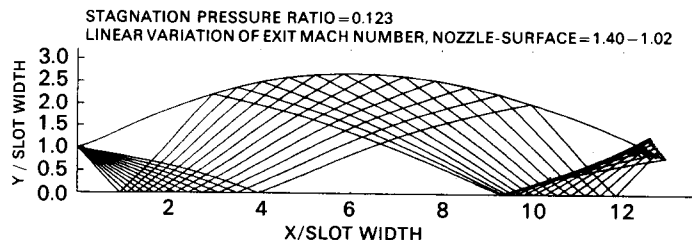


Figure 4 Variation of exit Mach number

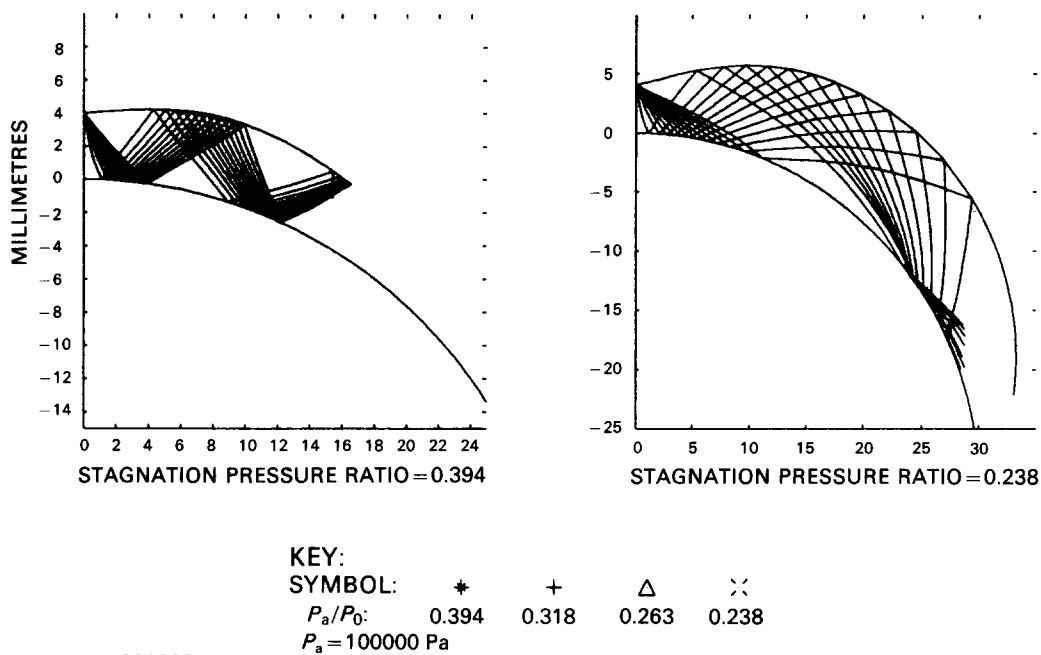


Figure 5 Jet over curved surface

Figure 6 shows a comparison with experiment for a high pressure ratio where the separated region is not visible. It shows the prediction overlaid onto a schlieren photograph of the flow. The free boundary of the prediction is seen to lie roughly in the middle of the shear layer. The expansion waves correspond to the white area, indicating falling density along the jet axis. The compressive reflections from the free surface correspond to the black region of rising density along the jet axis. At the end of the first cell (obscured by the overlay) the photograph shows a shock wave, which corresponds to the overlapping of the predicted compression waves.

Figure 7 shows the schlieren photograph close to breakaway conditions and may be compared with the low-pressure-ratio (0.238) pattern shown in Figure 5. There is a shock wave initiated by the start of the separation, and the subsequent cell structure is quite different from that predicted. A comparison of experimental and predicted surface static pressures is shown in Figure 8. For the highest pressure ratio, the separated region is fairly small. The initial expansion is predicted well, but the predicted minimum pressure is too low, and the pressure recovery appears too high. However, the experimental points are not close enough to determine the maximum pressure

recovery value with certainty. As the pressure ratio is reduced, the effect of the separation occurs before the minimum predicted pressure, which again is too low. The pressure rise is predicted much too steeply, and the recovery value is also too high. The lowest pressure ratio is close to the breakaway condition.

The effect of the ratio of slot width to Coanda radius of curvature is shown in Figure 9. This shows the predicted and measured static pressures for pressure ratios corresponding to near breakaway. The discrepancy is much more marked as the slot width is reduced. Note, however, that for the small slot width, a much higher upstream pressure (lower pressure ratio) is required for the jet to break away. Figure 10 shows the shadowgraph for the two slot widths, with the separated region being very large for the smallest slot width.

*Detached jet predictions*

In view of the strong effect of the separated region on the inviscid core of the jet, the modification to the program described earlier was made. Figure 11 shows the predicted jet pattern with the fit of the interpolated (predicted) pressure on the surface compared to the experimental points. One "guessed" or manually inserted



Figure 6 Schlieren,  $P_a/P_0=0.370$ , slot=4 mm

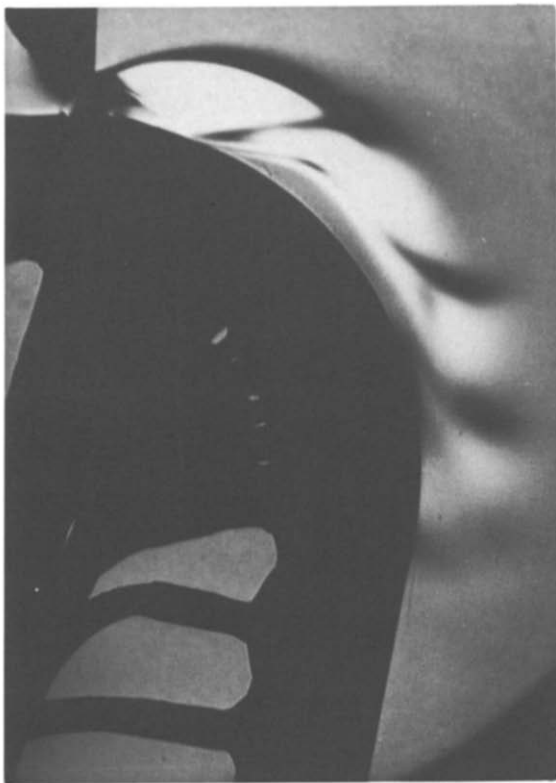


Figure 7 Schlieren,  $P_a/P_0=0.241$ , slot=4 mm

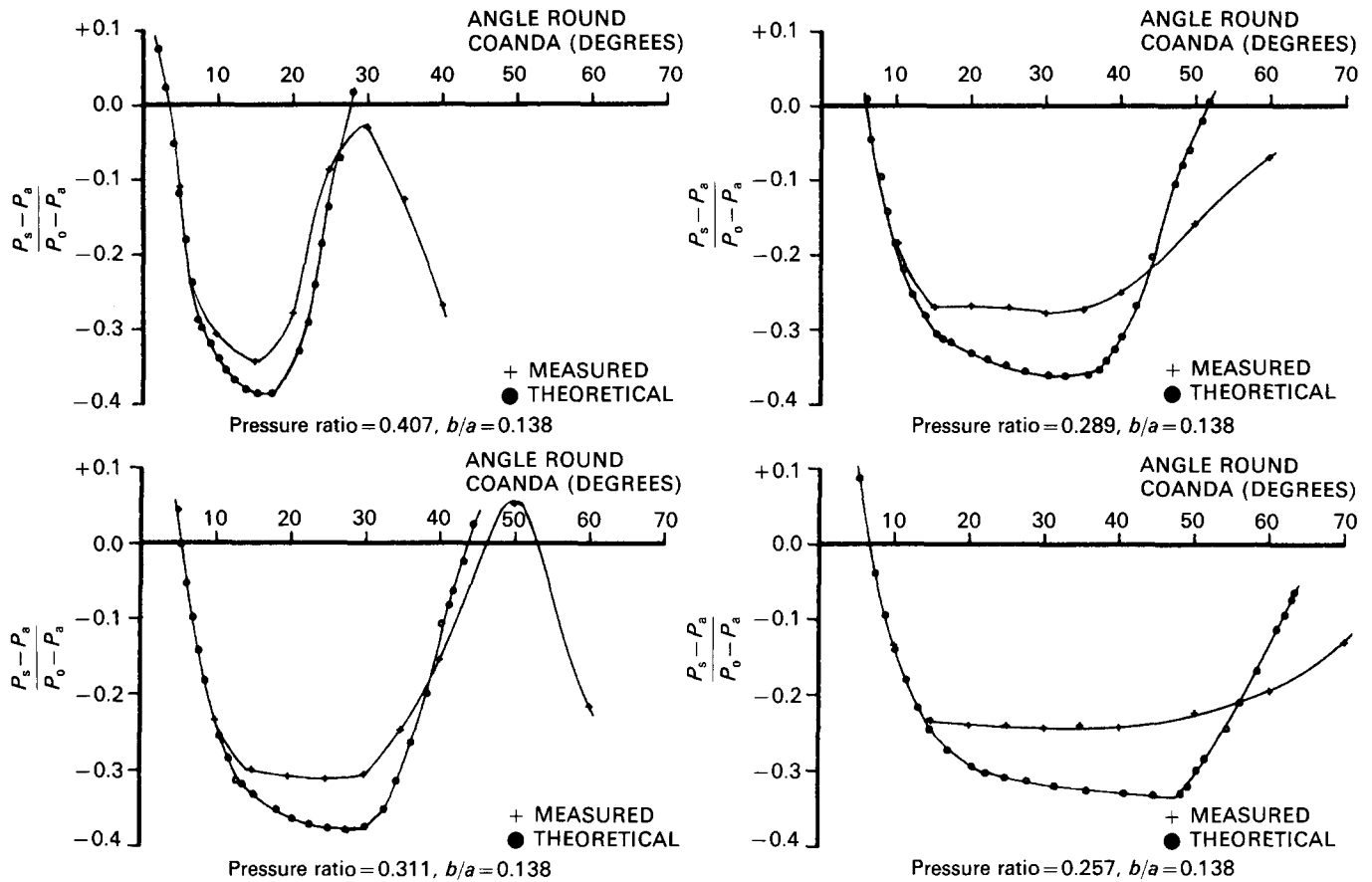


Figure 8 Comparison of surface static pressures

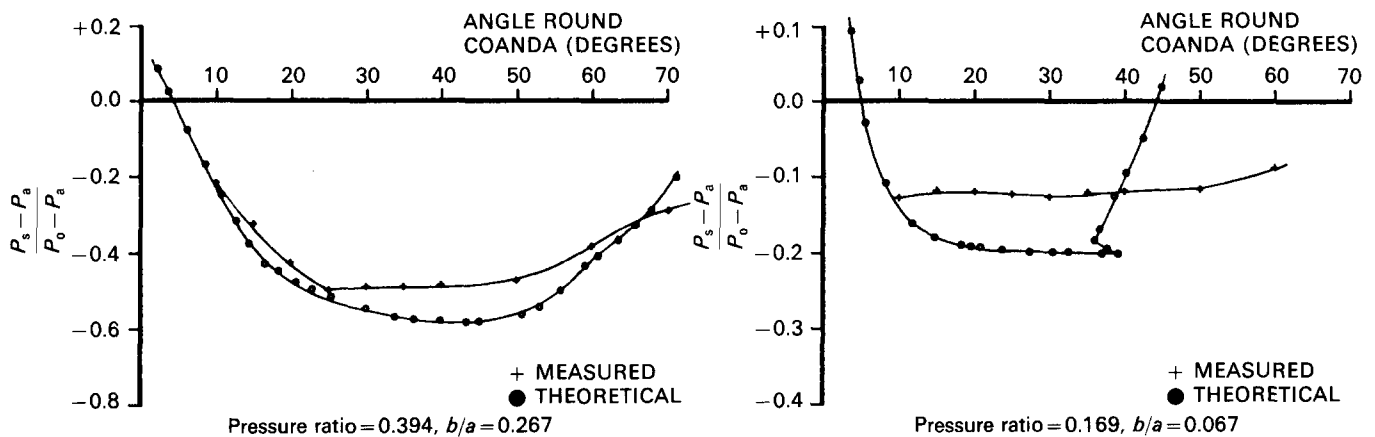


Figure 9 Surface static pressures near breakaway

point is shown. In view of some uncertainty in the pressure distribution between tapping points, some tests were made to see the effect of different "guessed" points. The results proved not to differ significantly. The prediction now shows strong compression, which in reality is an oblique shock from the start of the separated region, with a succession of shock cells downstream. The comparison with the schlieren photograph is shown in Figure 12, and the agreement with the overlaid prediction is remarkably good. The regions of rapid compression appear as dark shock waves on the photograph of vertical density gradients, with the inner and outer jet edges looking very reasonable.

The effect of slot width variation is seen in the predictions of

Figure 13, which may be compared with the shadowgraph pictures in Figure 10. The very much larger separated region with the small slot width is correctly predicted, with several shock cells downstream. Three cells are predicted, and these are seen in the shadowgraph picture at closely similar positions. For the large slot width, the smaller separation is seen, but it is predicted to start rather earlier than is observed.

### Conclusions

The method of characteristics is shown to be adequate for calculating the inviscid core of the underexpanded jet. However,

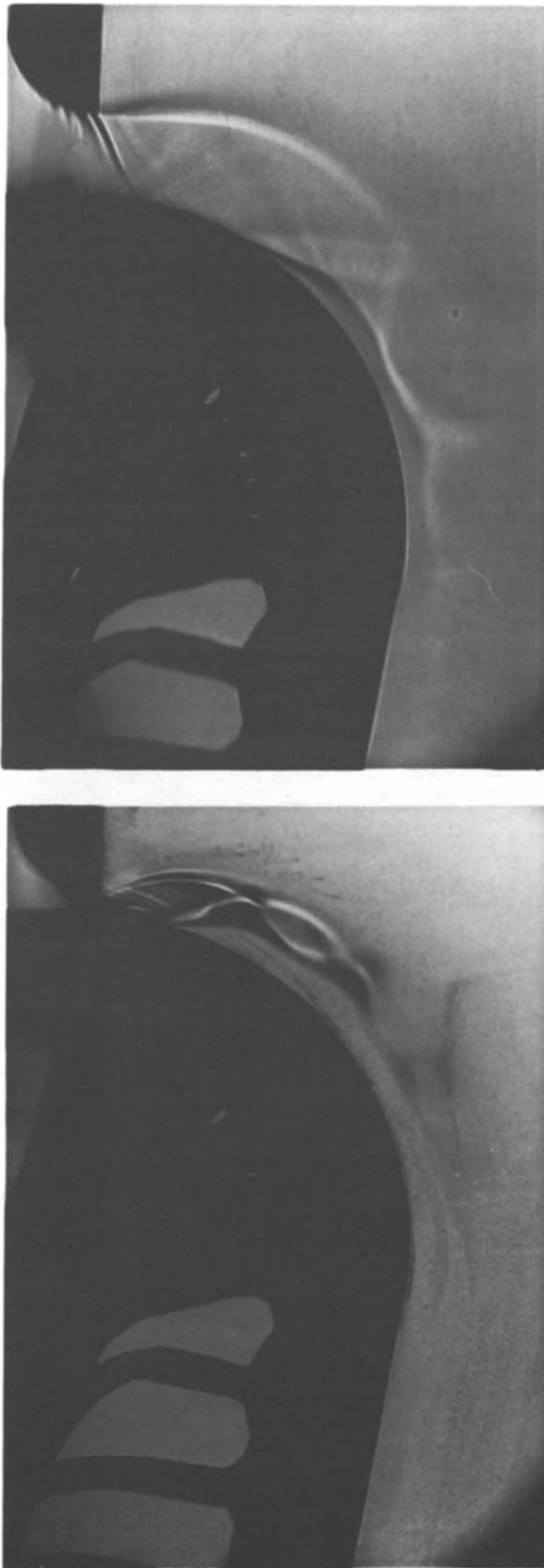


Figure 10 Jet near breakaway

for the curved wall jet the presence of a separated region alters the potential flow, the effect being greater as the upstream blowing pressure is increased. Thus the wall boundary condition has to be replaced by a condition which allows for this separated region. The method chosen here is to use measured

static pressures along the curved surface, and thus have a specified pressure boundary. The prediction gives good results when compared with the observed flow pattern, in spite of the neglect of the shear layers. The small effect of the shear layers is because the area of interest is the first one or two shock cells. Further downstream the prediction either failed because the flow became subsonic, or it became progressively less accurate as the shear layer encroached into the inviscid core.

The core calculation method is effectively the first step in a combined viscid-inviscid jet calculation, along the lines suggested by Dash *et al.*<sup>6</sup> However the calculation of the separated region will be fairly complex, since the flow separation and reattachment will probably be in the transitional regime between laminar and turbulent flow. The effect of the outer shear layer will also need to be included so that calculation of

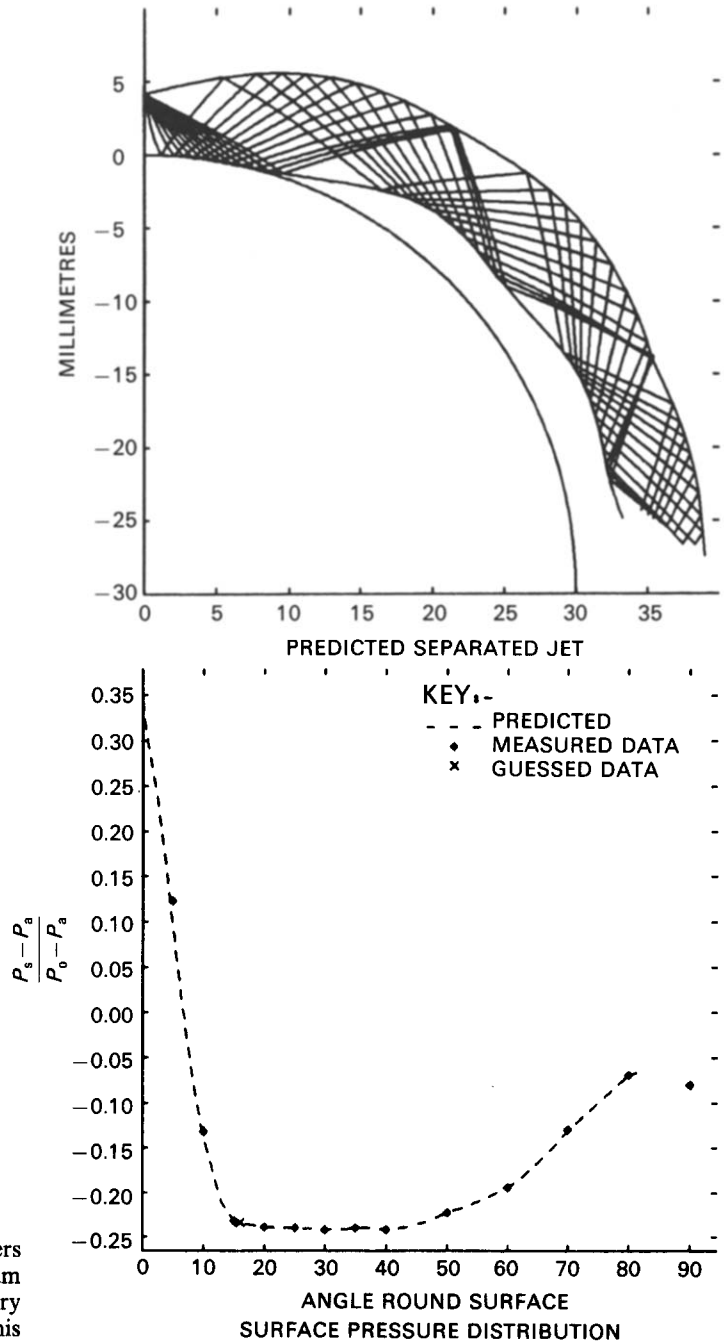


Figure 11 Separated jet,  $b/a=0.138$ ,  $P_s/P_0=0.257$



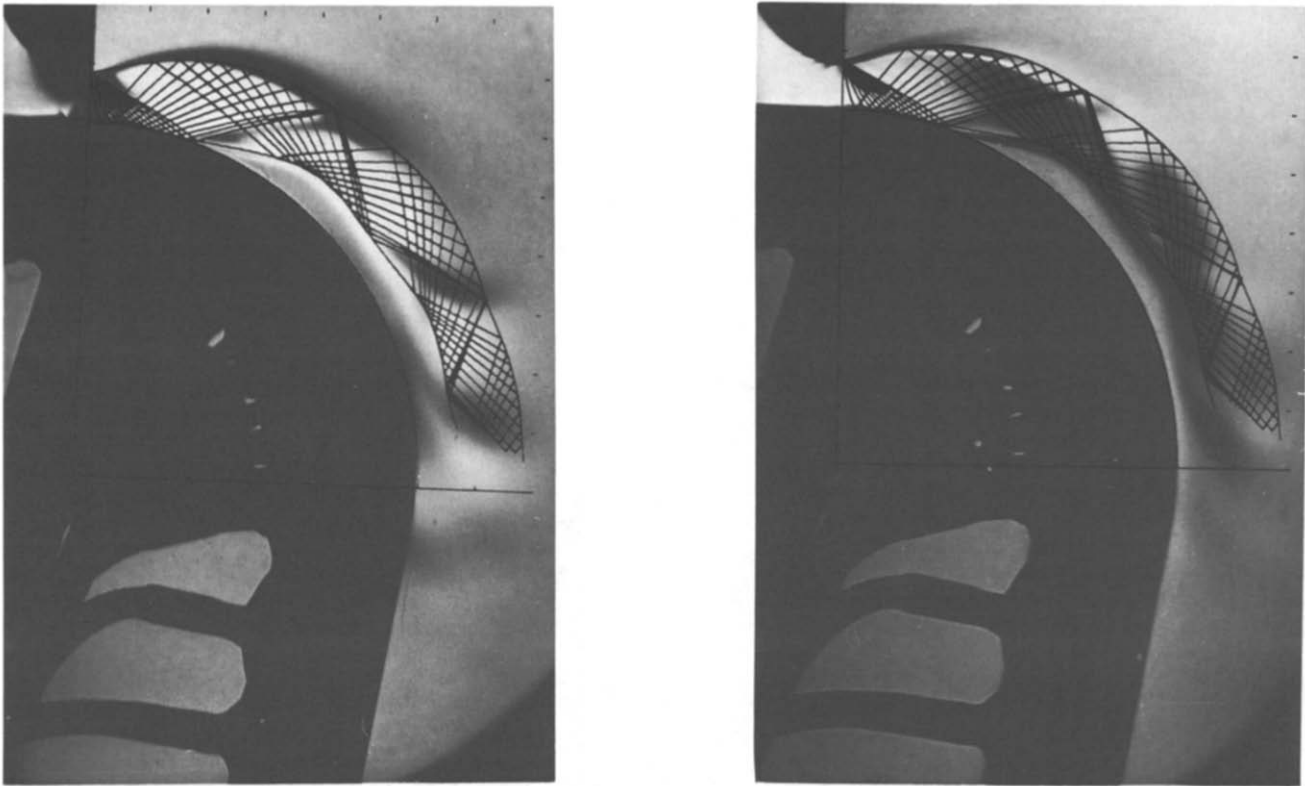


Figure 12 Comparison of Schlieren and calculation

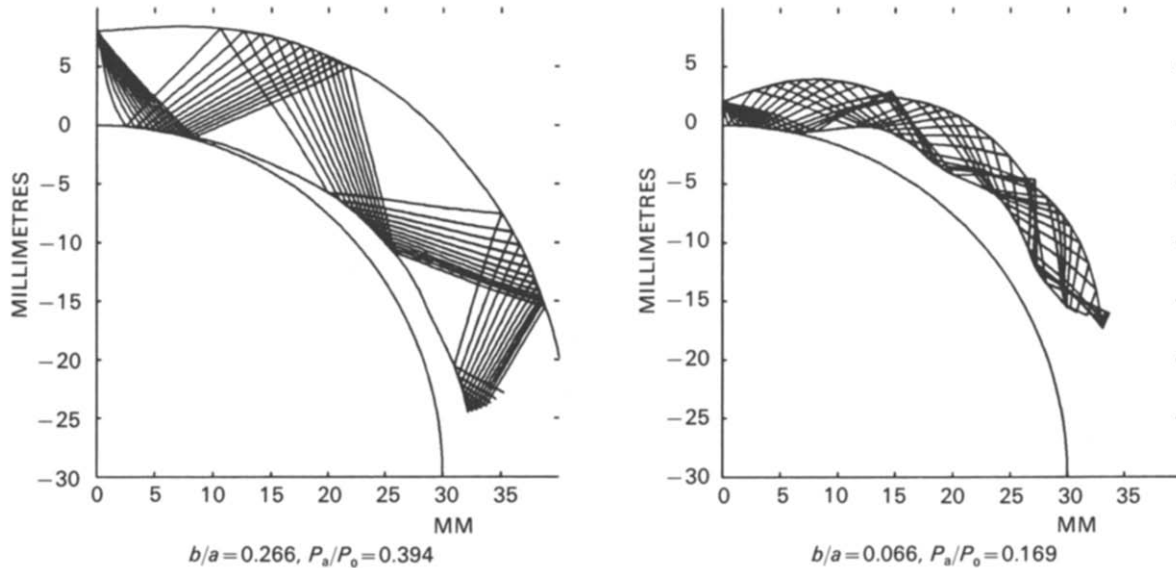


Figure 13 Jet predictions near breakaway

the jet to the fully developed subsonic region can be performed. This is important for the Coanda flare application where air entrainment and downstream velocity profiles are needed for combustion considerations.

As regards breakaway, the present method gives some guidance in that experimentally it was found that breakaway occurred when the pressure recovery reached a position of about  $70^\circ$ . The prediction method gives some indication as to where this will take place, except for the smallest slot width. However the inclusion of the calculation of the separated region is

required for a prediction method that will give breakaway accurately.

The two-dimensional method will be applicable to some situations, but for the Coanda flare, the work needs extension to axisymmetric flow. The axisymmetric jet is known to break away at higher blowing pressure (Gilchrist<sup>10</sup>), due to thinning of the jet by the radially outward flow. There may be additional complications due to longitudinal vortices for which there is some evidence in the fully developed jet (Morrison<sup>12</sup>), but as regards breakaway, these are not likely to be important.

## Acknowledgment

The authors acknowledge the support of British Petroleum plc and the S.E.R.C. for this work.

## References

- 1 Gregory-Smith, D. G. and Gilchrist, A. R. The compressible Coanda wall jet: an experimental study of jet structure and breakaway. *Int. J. Heat Fluid Flow*, 1987, **8**, 156–164
- 2 Wilkins, J., Withridge, R. E., Desty, D. H., Mason, J. T. M., and Newby, N. The design and development and performance of Indair and Mardair flares. Offshore Technology Conference, 1977, Houston, paper No. 2822
- 3 Morrison, J. F. and Gregory-Smith, D. G. Calculation of an axisymmetric turbulent wall jet over a surface of convex curvature. *Int. J. Heat Fluid Flow*, 1984, **5**, 139–148
- 4 Spalding, D. B. Genmix—a general computer program for two-dimensional parabolic phenomena. *Science and Applications of Heat and Mass Transfer*, Vol. 1, 1977. Pergamon Press
- 5 Gibson, M. M. and Younis, B. A. Modelling the curved turbulent wall jet. *AIAA J.*, 1982, **20**, 1707–1712
- 6 Dash, S. M., Beddini, R. A., Wolf, D. E., and Sinha, N. Viscous/inviscid analysis of curved sub- or supersonic wall jets. AIAA 16th Fluid and Plasma Dynamics Conf., 1983, No. AIAA-83-1679
- 7 Chang, I-S. and Chow, W. L. Mach disc from underexpanded axisymmetric nozzle flow. *AIAA J.*, 1974, **12**, 1079–1082
- 8 Benson, R. S. and Poole, D. E. Compressible flow through a two-dimensional slit. *Int. J. Mech. Sci.*, 1965, **7**, 315–336
- 9 Zuchrow, M. J. and Hoffman, J. D. *Gas Dynamics*, Vols. 1, 2. Wiley, New York, 1976
- 10 Gilchrist, A. R. The development and breakaway of a compressible air jet with streamline curvature and its application to the Coanda flare. Ph.D. Thesis, Durham University, 1985
- 11 Hoffman, J. D. Accuracy studies of the numerical method of characteristics for axisymmetric steady supersonic flow. *J. Comp. Phys.*, 1973, **11**, 210–239
- 12 Morrison, J. F. A study of the axisymmetric wall jet with streamline curvature and its application to the Coanda flare. Ph.D. Thesis, Durham University, 1982